



Ferrari-John, R.S. and Batchelor, A.R. and Katrib, Juliano and Dodds, Chris and Kingman, S.W. (2016) Understanding selectivity in radio frequency and microwave sorting of porphyry copper ores. *International Journal of Mineral Processing*, 155 . pp. 64-73. ISSN 0301-7516

**Access from the University of Nottingham repository:**

<http://eprints.nottingham.ac.uk/35949/1/MP-16-299%20Manuscript%20%28REVISED%29.pdf>

**Copyright and reuse:**

The Nottingham ePrints service makes this work by researchers of the University of Nottingham available open access under the following conditions.

This article is made available under the University of Nottingham End User licence and may be reused according to the conditions of the licence. For more details see: [http://eprints.nottingham.ac.uk/end\\_user\\_agreement.pdf](http://eprints.nottingham.ac.uk/end_user_agreement.pdf)

**A note on versions:**

The version presented here may differ from the published version or from the version of record. If you wish to cite this item you are advised to consult the publisher's version. Please see the repository url above for details on accessing the published version and note that access may require a subscription.

For more information, please contact [eprints@nottingham.ac.uk](mailto:eprints@nottingham.ac.uk)

# 1 **Understanding selectivity in radio frequency and microwave sorting of porphyry copper ores**

2 R.S. Ferrari-John\*, A.R. Batchelor, J. Katrib, C. Dodds, S.W. Kingman

3 Department of Chemical and Environmental Engineering, University of Nottingham, University Park,  
4 Nottingham, NG7 2RD, United Kingdom

5 \* Corresponding author. E-mail address: becca.john@nottingham.ac.uk (R.S Ferrari-John)

6

## 7 **Abstract**

8 Continuous high-throughput microwave treatment followed by infrared thermal imaging (MW-IR) has  
9 previously been shown to provide attractive separations for a number of porphyry copper ores, leading to  
10 rejection of a large proportion of barren fragments from ore-grade material or concentration of copper values  
11 from waste-grade material. However, the efficacy of the sorting process is reduced by the presence of  
12 hydrated clays and pyrite. Literature measurements have shown differences in the conductivity of pyrite and  
13 copper sulphides such as chalcopyrite at radio frequencies. In this work the potential of using radio frequency  
14 (RF) heating to exploit these differences and achieve improved selectivity between copper and iron sulphides,  
15 is investigated. For the first time a novel bulk materials handling and presentation method that facilitates even  
16 heating of angular ore fragments in parallel plate RF systems is discussed. The fragment-by-fragment thermal  
17 response of five ore samples under equivalent pilot MW-IR and RF-IR processing conditions is evaluated,  
18 showing that there is an increase in selectivity in the heating of hydrated clay minerals in RF compared to  
19 microwave. It is suggested, again for the first time, that selectivity in the microwave processing of ores  
20 containing semi-conducting minerals is due predominantly to magnetic absorption (induction heating) caused  
21 by eddy currents associated with the magnetic field component of electromagnetic energy. In radio frequency  
22 processing, where electric field is the dominant component, heating of semi-conducting minerals is limited by  
23 the electric field screening effect. This effect is demonstrated using synthetic fragments. Thermal response  
24 profiles of synthetic fragments show that approximately 2.5 times the mass of sulphide minerals to hydrated  
25 clay minerals would result in an equal temperature increase for microwave heated fragments in which the  
26 microwave-heating minerals are evenly disseminated throughout the matrix. This understanding provides the  
27 foundations for development of models incorporating different thermal responses for individual heated phases,  
28 alongside other textural and treatment variables, that can be used to predict how close to intrinsic sortability  
29 ores will perform in MW-IR and RF-IR without the need for extensive processing trials.

## 30 **Keywords**

31 microwave, radio frequency, ore, copper, sorting, infrared

## 32 1 Introduction

33 In recent years sorting of ores has seen renewed interest, as a means of reducing comminution energy, with  
34 many studies demonstrating the potential benefits of applying sensor based sorting to mineral processing  
35 operations (Tong et al., 2015, Norgate and Jahanshahi, 2010, van Berkel, 2007, Pokrajcic et al., 2009,  
36 Lessard et al., 2014). For large scale, low grade operations such as porphyry copper processing, pre-  
37 concentration to reject uneconomic material prior to the energy intensive grinding stages has the potential to  
38 significantly improve the sustainability of operations. These improvements could be realised by an increase in  
39 the grade to the concentrator (and therefore copper output) and a reduction in the copper specific energy  
40 consumption in comminution and water usage in processing (Salter and Wyatt, 1991). Sensor based sorting  
41 on a fragment by fragment basis also provides an opportunity to scavenge valuable material from waste; the  
42 extent of waste as a resource was demonstrated in a study by Klein and Mazhary (2015) which showed that  
43 25% of waste dump material from two porphyry deposits was of a high enough grade to be economically  
44 processed. Key to unlocking the potential of ore sorting is selection of appropriate discrimination sensor  
45 technologies. Many sensors currently proven at industrial throughputs rely on surface techniques, which for  
46 highly heterogeneous ores such as those found in porphyry copper deposits, do not give suitable separations  
47 for sorting (Tong et al., 2015).

48 Microwave heating followed by infra-red thermal imaging (MW-IR) has been investigated as a potential  
49 excitation-discrimination technique for sorting of ores (Van Weert and Kondos, 2008, Van Weert et al., 2011,  
50 John et al., 2015, Ghosh et al., 2013, Ghosh et al., 2014). Microwave energy provides selective and  
51 volumetric heating of certain mineral phases within the ore matrix; semi-conductive minerals such as nickel,  
52 copper, iron and lead sulphides, oxides such as magnetite and other minerals with bound and/or free water  
53 (e.g. smectite clay) heat far more readily than common rock-forming minerals, such as quartz, feldspars,  
54 calcite and micas (Walkiewicz, 1988, McGill et al., 1995, Chunpeng and Yixin, 1996, Harrison, 1997).  
55 Measurement of individual surface average temperature of fragments then provides a basis for discriminating  
56 between valuable and uneconomic material.

57 The pilot scale sorting performance of 16 porphyry copper ores has been investigated using a high throughput  
58 100t/h belt based 100 kW microwave system designed to operate together with commercially available sorting  
59 modules (Batchelor et al., 2016). Overall, the best performing ores under MW-IR were those with a low  
60 average moisture content and co-mineralisation of copper and iron sulphides. On the other hand, abundance  
61 of microwave heating gangue minerals, such as iron sulphides, iron oxides and hydrated clays, reduced the  
62 efficacy of the sorting process.

63 Radio frequency electromagnetic energy is longer in wavelength than microwave energy; for the relevant  
64 industrial, scientific and medical (ISM) bands this difference equates to 11m at 27.12 MHz RF compared to  
65 33cm at 896 MHz microwave. The electromagnetic heating properties of materials vary with frequency.  
66 Measurements of the radio frequency conductivities of selected sulphides and iron oxides by Genn and  
67 Morrison (2014) suggest favourable differences between the electromagnetic heating of copper and iron  
68 sulphide minerals may be observed at radio frequencies, compared to the microwave range. These measured  
69 differences in conductivity of pyrite and chalcopyrite suggest that electromagnetic processing of porphyry  
70 copper ore fragments at radio frequencies rather than microwave frequencies should lead to increased  
71 heating of chalcopyrite compared to pyrite. Achieving this improved selectivity during the sorting process could  
72 lead to sortability performance for ores closer to their intrinsic potential. However, the effect of varying  
73 electromagnetic frequency, specifically the use of radio frequency (RF) excitation has not been considered in  
74 the literature with respect to ore sorting based on heating effects.

75 The objective of this paper is to determine for the first time the potential of using RF-IR excitation-  
76 discrimination to sort porphyry copper ores on a fragment by fragment basis and investigate whether improved  
77 selectivity of copper sulphide minerals can be achieved compared to MW-IR. A novel method for materials  
78 handling during bulk RF excitation is developed that allows the fragment-by-fragment thermal response  
79 following microwave and RF treatment to be evaluated. Using this method the difference in the thermal  
80 response of fragments during microwave and RF processing is determined and evaluated with respect to the  
81 mineralogy of the ore fragments. Using synthetic fragments, the electric and magnetic field contributions to the  
82 overall heating of sulphide and clay minerals at microwave and radio frequencies are evaluated, and the  
83 implications these findings have for optimising selectivity in industrial scale ore sorting based on MW or RF-IR  
84 excitation and discrimination are discussed.

85

## 86 **2 Materials and methods**

### 87 *2.1 Sample mineralogy, preparation and characterisation*

88 Five porphyry copper ore samples were processed in this investigation, all originating from the same host site.  
89 The five samples were two ore and two waste grade feeds with varying lithologies, plus a recycled pebbles  
90 sample. Bulk ore samples (~200kg) were supplied in three narrow size classes, namely -65.5+50.8mm, -  
91 50.8+25.4mm and -25.4+12.7mm. These size classes are based on the requirements for compressed air jets  
92 that would be used to blast fragments during separation in industrial ore sorting processes. Each 200kg barrel  
93 was split using a rotary sample divider to provide sub samples of 240 fragments. Each fragment was heated  
94 individually in a microwave cavity and infra-red images for each fragment analysed. Each fragment was then  
95 cut in half and each half retested in the microwave; if each half was shown to have equivalent thermal  
96 responses the fragment progressed to the next stage of preparation. For equivalent halves, one was kept for  
97 sorting tests whilst the other was pulverised to -75 $\mu$ m to produce powders for elemental and moisture  
98 analysis. For each ore type tested, a set of 72 fragments were produced across the three size classes and  
99 were selected to give a range of thermal responses. The samples were produced in this manner to be  
100 indicative of the extremities of thermal responses that could be observed within a particular ore. Fragments  
101 were classified according to copper content and temperature rise within the wider test sample. For each ore  
102 sample, the hottest 30% of fragments by mass and the richest (Cu) 30% by mass were used to determine  
103 response thresholds, and fragments classified as true negative, false negative, true positive and false positive.  
104 For example true negatives were low copper content fragments (lowest 70% Cu by mass) that exhibited a low  
105 temperature rise (coldest 70% by mass). This selection methodology minimised the number of fragments with  
106 very complex compositions, allowing the mineralogical reasons for thermal responses to be elucidated.  
107 However because of the selection method used, it should be noted that the sample grade and thermal  
108 responses are not representative of the bulk ore as a whole. Individual fragment copper, sulfur and iron  
109 content were determined using powder XRF. Chalcopyrite and pyrite content for each fragment was  
110 calculated from stoichiometry, assuming these were the only sulphides present (see Table 1). Moisture  
111 analysis was performed using thermo-gravimetric analysis (TGA) to heat a small sub-sample (~20mg) of the  
112 pulps to 120°C. The sample was held at 120°C for 5 minutes to allow the vast majority of the free water to be  
113 driven off. 120°C was chosen to remove the vast majority of free water without altering the chemical structure  
114 of the clays. Moisture analysis reproducibility testing of five subsamples from a single ore fragment yielded a  
115 standard deviation of 6.6% between measurements ( $0.380 \pm 0.025$  Wt%) which was deemed sufficient for the  
116 purposes of this investigation.

117

**Table 1 Ore lithology and major heated phase content**

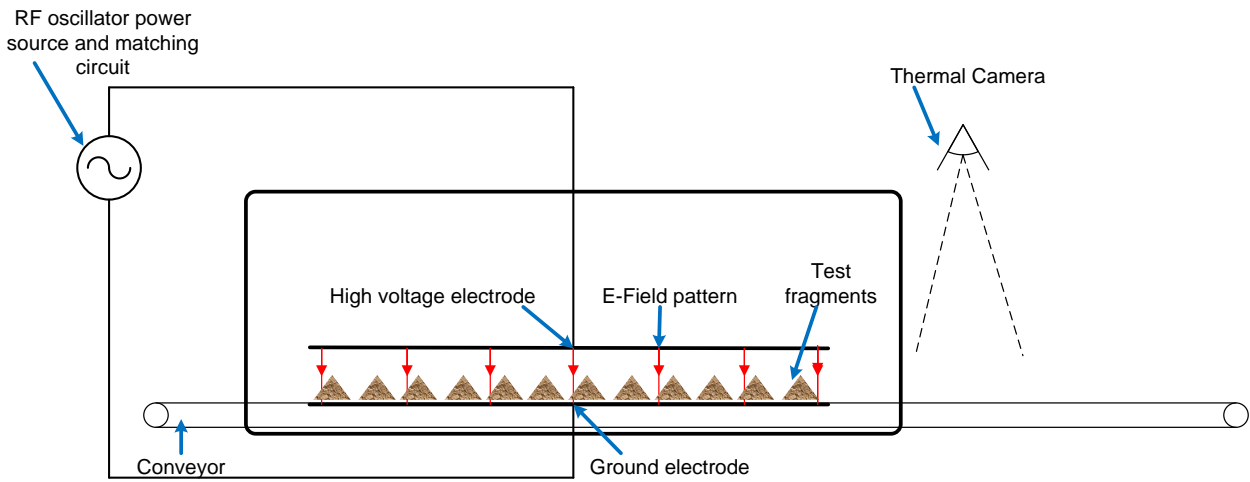
Ore	Lithology	Chalcopyrite Average Weight %	Pyrite Average Weight %	Free water Average Weight %	Total Average Weight %
1	Limestone Skarn	0.90	10.45	0.49	11.85
2	Quartzite (Waste)	0.75	1.99	0.20	2.93
3	Quartz-monzonite	1.57	5.34	0.27	7.18
4	Quartz-monzonite (Waste)	0.50	3.25	0.70	4.46
5	Recycled pebbles	0.56	1.47	0.72	2.75

## 120 2.2 Pilot scale continuous MW treatment of ores

121 Continuous microwave treatment of samples was carried out using the pilot scale 100kW 896 MHz system  
 122 and processing methodology described in detail in (Batchelor et al., 2016). The test fragments were spread  
 123 across the full width of the microwave belt in a closed monolayer (100% belt coverage) arrangement within a  
 124 bed of fill material of the same ore. The fill material was chosen to be the -50.8+25.4mm size class as this  
 125 most closely approximated the average size of the 72 test fragments in each sample. Fragments were treated  
 126 in two different orientations at target microwave energy inputs of 0.7 kWh/t. This dose was achieved by  
 127 selection on an appropriate belt mass loading, belt speed and microwave power for each ore.

## 128 2.3 Pilot scale batch RF treatment of ores

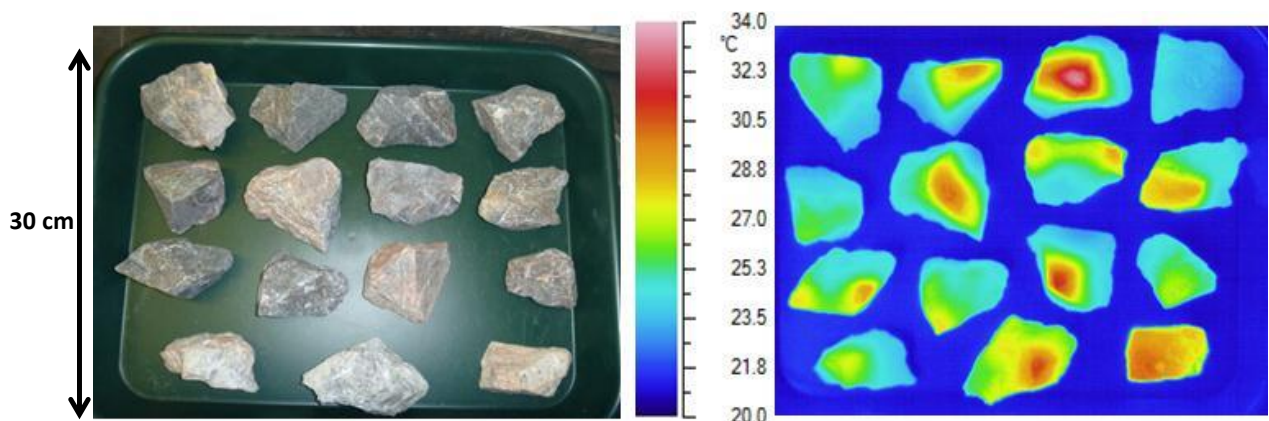
129 Radio frequency testing of ores and synthetic fragments was carried out in a 20kW 27 MHz Sairem 50Ω radio  
 130 frequency system. The system provides a highly homogenous electric field between two parallel plate  
 131 electrodes measuring 440x1200mm. Test fragments were placed in a plastic tray in the chosen orientation.  
 132 Three trays of sacrificial material were used to fill the remaining belt space between the RF electrodes. Fill  
 133 material was of the same ore as the test sample, and the size class was chosen to closely match the height of  
 134 the test fragments. The total mass of ore in each tray of fill material was kept within ±5% of the mass of the  
 135 test fragments sample tray, to minimise changes in treatment times and provide an even load between the  
 136 electrodes. The electrode height was fixed at 5mm above the tallest fragment. A vector network analyser  
 137 (VNA) was used to pre-match the impedance of the load and the RF generator, to determine parasitic losses  
 138 and maximise absorbed power. Fragments were treated statically between the electrodes for a set exposure  
 139 time and power, to give the required dose of 0.7 to 1.0 kWh/t. Parasitic energy losses within the system were  
 140 <2% and therefore assumed to be negligible. Power absorbed into the ore was calculated as the difference  
 141 between forward and reflected power. Figure 1 presents a schematic of the monolayer treatment.



142  
143 **Figure 1: RF treatment apparatus for batch monolayer testing**

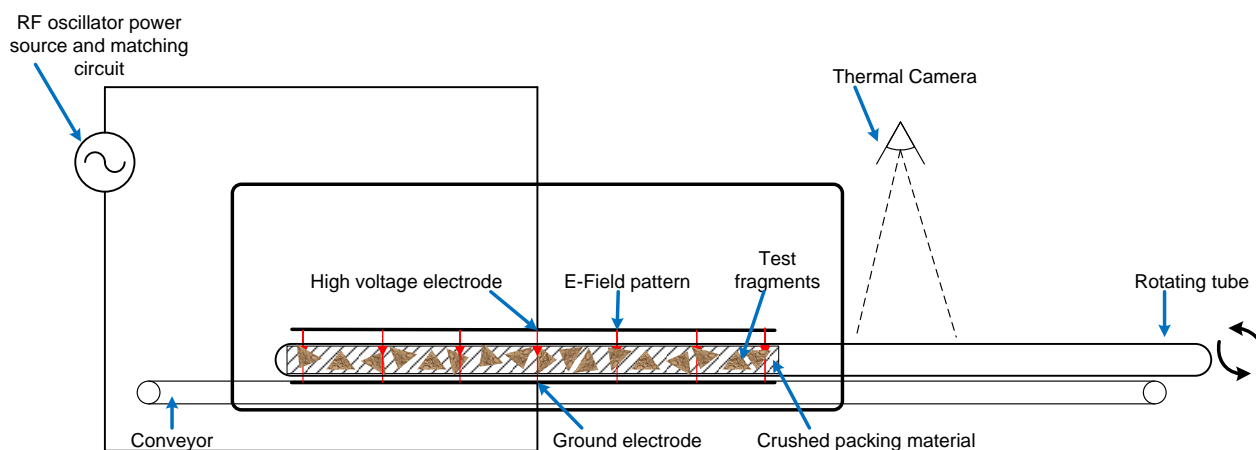
144 *2.3.1 Developing a method for fragment presentation in RF treatment*

145 It was observed during initial scoping tests of ore fragment monolayers in the RF parallel plate system that hot  
 146 points were occurring on the edges and tips of fragments located closest to the upper electrode. Ferrari-John  
 147 et al. (2016) conducted an investigation into the specific effects of geometry on the heating profiles of irregular  
 148 shaped loads. The presence of edges and vertices on angular particles, and their proximity to faces  
 149 perpendicular to RF parallel plate electrodes, increased localised heating, due to electric field concentrations  
 150 at these locations. For angular particles with homogenous dielectric properties, this localised heating was  
 151 shown to dominate temperature rise; particles of the same geometry processed in different orientations  
 152 exhibited different heating profiles (Ferrari-John et al., 2016). This effect in the heating of ore fragments is  
 153 shown in Figure 2. A fragment thermal response related to angularity and orientation rather than mineral  
 154 content in an RF-IR sorting process would have a negative impact on actual sortability performance. To use  
 155 RF-IR to discriminate between ore fragments based on mineralogical composition rather than geometry,  
 156 development of a method to overcome these shape effects was required.



157  
158 **Figure 2 Sample photo and IR thermal image of angular fragments following monolayer treatment in**  
 159 **parallel plate RF system**

160 A method for rotating a packed bed of material within the RF cavity was devised that was found to largely  
 161 mitigate the effect of fragment geometry. The test fragments were placed in a cylindrical plastic tube and  
 162 surrounded by crushed fill of the same ore type to cover the full length of the electrodes. The sample tube was  
 163 plugged to prevent any spillage or movement of the packed bed during treatment. An empty length of the  
 164 sample tube extended out of the RF tunnel so the tube could be manually rotated during treatment. By  
 165 surrounding the test fragments with crushed fill material of the same ore type, electric field concentrations on  
 166 tips and edges are minimized as power is absorbed into the surrounding material as well as the test  
 167 fragments. By also rotating the bed of material (at approximately 15 rpm), tips and edges are no longer in a  
 168 static position and the presentation of the fragments to the electric field is constantly changing. Tubes of  
 169 sacrificial material of the same ore type and mass were placed alongside the sample tube in the tunnel to  
 170 provide an even load between the electrodes. Total energy input was scaled by increasing the treatment time,  
 171 and power, to provide a comparative energy dose to monolayer treatments. The rotating packed bed testing  
 172 schematic is presented in Figure 3.



173

174

**Figure 3: RF treatment apparatus for batch rotating packed bed testing**

175

#### 2.4 Thermal image analysis

176

The thermal response of ore and synthetic fragments following microwave or RF treatment was captured using an NEC H2640 thermal imaging camera. For each recorded test run with any excitation method, a thermal image was taken immediately prior to treatment. After treatment, thermal images were captured for 2 minutes at 1 frame per second to record thermal bloom and dissipation in each individual sample. Thermal images were recorded and analysed via Radiometric Complete Online (Radiometric Infrared Solutions, 2011). Average temperature rise was used as the basis for analysis, as maximum temperature rise only corresponds to the hottest pixel measured. For all tests, the recorded frame corresponding to a measurement delay time of

182



183 45s was selected for comparison as this was the shortest common delay time across all samples tested for all  
184 treatment methods.

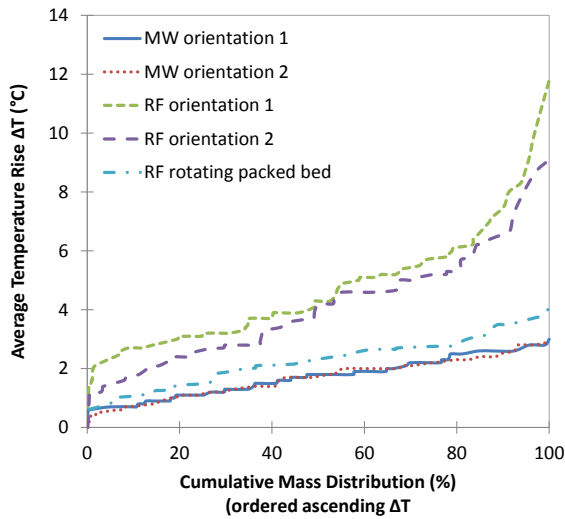
## 185 *2.5 Calculating ore sortability performance*

186 The sorting performance of each ore sample was determined by plotting ore sortability curves. These are  
187 analogous to the grade/mass recovery curves, used to assess the performance of flotation circuits.  
188 Metallurgical efficiency of a concentration process can be expressed by a curve showing the recovery  
189 attainable at any value of concentrate grade (Wills et al., 2006). In the case of electromagnetic ore sorting  
190 with infrared imaging (EM-IR), the concentrate grade is the grade of 'hot' fragments that have been accepted  
191 during sorting. An intrinsic sortability curve of an ore sample is determined by ordering fragments from  
192 highest to lowest copper grade. The cumulative grade (or cumulative copper recovery) can then be  
193 determined on a fragment by fragment basis (Tucker et al., 2013), and for different mass recoveries.

### 194 **3 Comparing MW-IR and RF-IR sorting**

#### 195 *3.1 The influence of processing method and presentation on fragment thermal response*

196 Previous work (Batchelor et al., 2016) showed that for microwave sorting treatments, energy dose was the  
197 single most important variable for controlling the average temperature rise of fragments. In this work, the  
198 microwave or RF energy input has been kept constant for treatment each ore sample under equivalent  
199 conditions (between 0.7 and 1.0 kWh/t) to investigate whether there is improved selectivity in the heating of  
200 target minerals at radio frequency compared to microwave. The effects of processing method (microwave or  
201 RF) and fragment presentation (orientation 1 or 2, or rotating packed bed treatment with IR measurement in  
202 orientation 1) on average temperature rise under equivalent treatment conditions are illustrated for Ore 3, the  
203 quartz-monzonite sample, in Figure 4 (the results for all samples are shown in S1 in of the Supplementary  
204 Information). All treatments were performed at a target electromagnetic energy dose of 0.7kWh/t. For Ore 3,  
205 under microwave treatment conditions, the thermal response profile of the fragments is similar in both  
206 orientation 1 and orientation 2. The influence of fragment orientation in pilot scale microwave treatment was  
207 previously shown to have no adverse effect on sortability performance, as it did not make a hot fragment  
208 appear cold or vice versa (Batchelor et al., 2016). However, for RF monolayer treatments at equivalent dose,  
209 the average temperature rise for all fragments is higher. This is expected due to the uneven heating in the RF  
210 system for fragment tips closest to the electrodes, however these effects were observed to be more extreme  
211 in Ore 3 compared to other samples due to the increased angularity. The RF rotating packed bed treatments  
212 were undertaken to mitigate this effect. For Ore 3 and equivalent energy inputs, the thermal response profile is  
213 closer to that observed in microwave testing. The thermal responses of fragments in packed beds rather than  
214 monolayers will therefore be used for comparison with microwave treatments of ores for the remainder of this  
215 section.



216

217  
218

**Figure 4: Ore 3 variation in ore thermal response profile due to fragment presentation method and frequency**

219

220

221

222

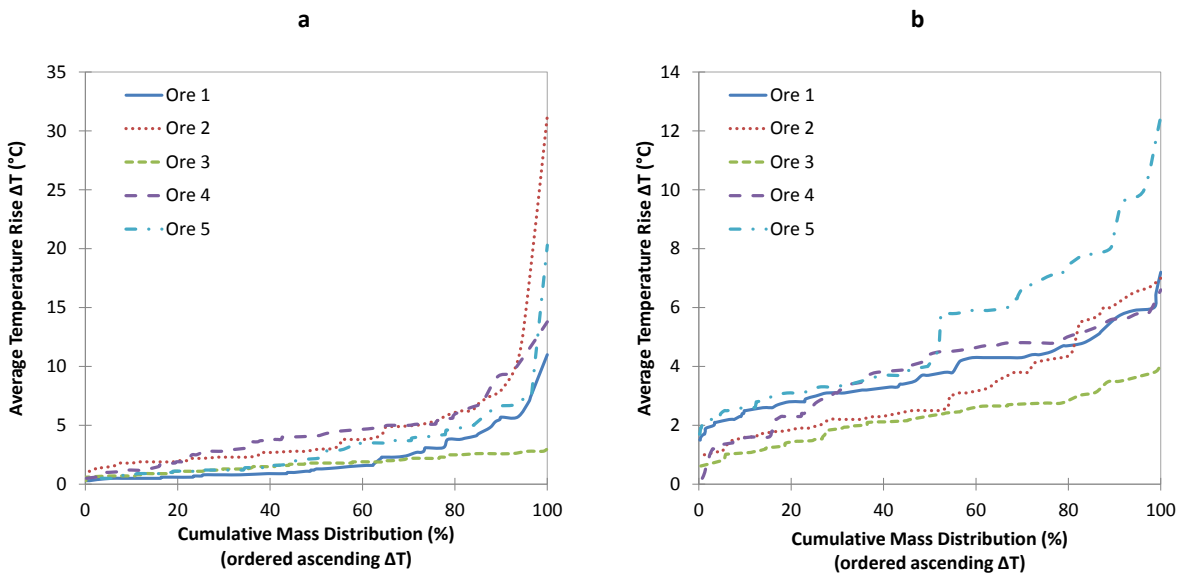
223

224

225

226

The variation in fragment thermal response profiles for the five different ore samples tested are illustrated in Figure 5, for microwave orientation 1 and RF rotating packed bed treatments. The range of thermal responses observed is much greater for microwave treatment compared to RF treatment. With maximum individual fragment temperatures of over 30°C for microwave treatment, but only 12°C for RF rotating packed bed treatment. Given that treatments are carried out at equivalent energy dose, this suggests a difference in the selective heating of the different mineral phases between microwave treatment at 896 MHz and RF treatment at 27 MHz. Furthermore the relative order of the different ores varies, with Ore 2 exhibiting the highest average temperature rise in microwave and Ore 5 the highest in RF rotating packed bed.



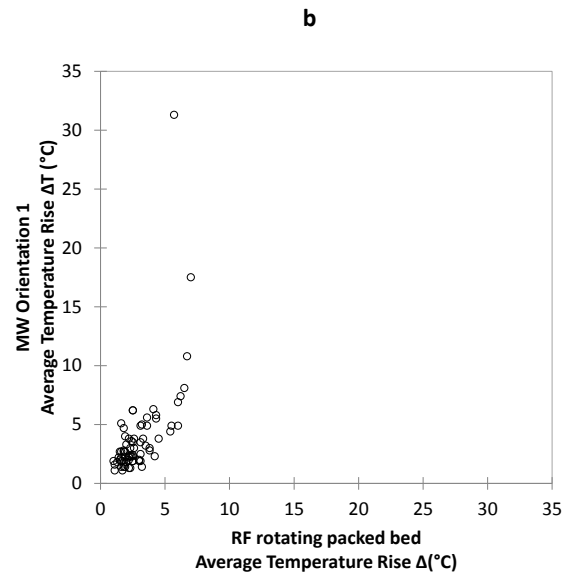
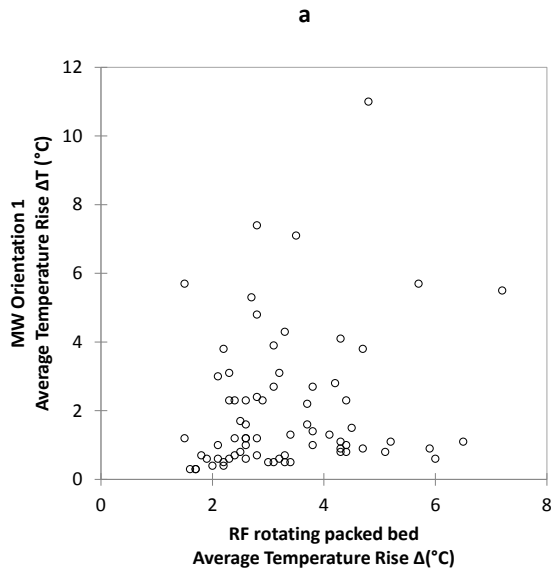
227

228  
229

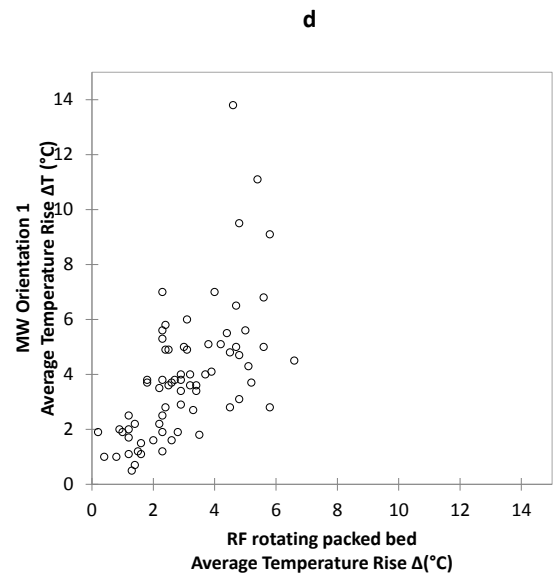
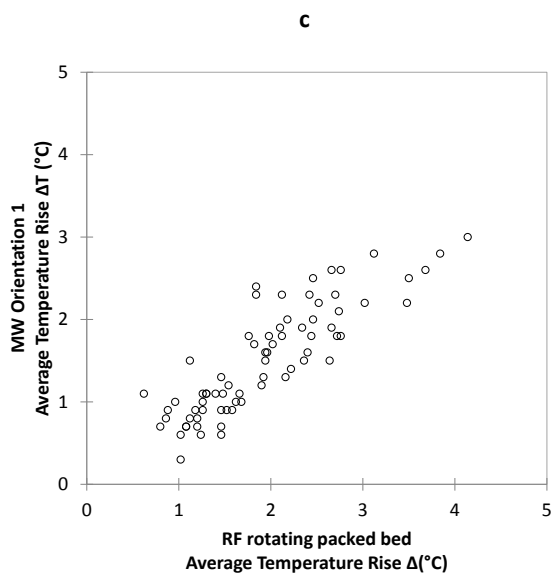
**Figure 5: MW orientation 1 (a) and RF rotating packed bed (b) variation in thermal response profiles due to ore type**

230

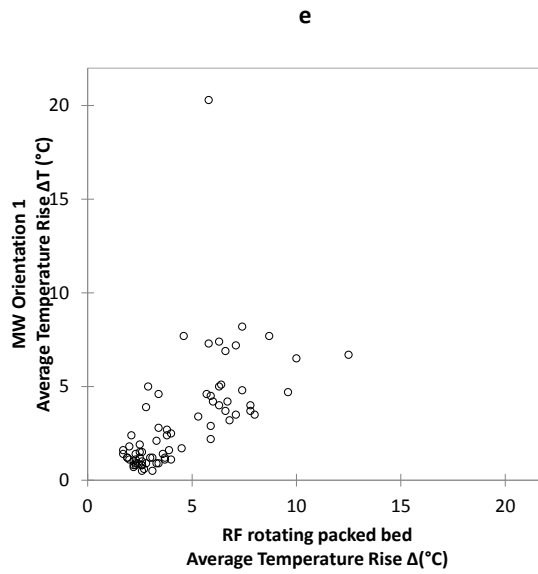
231 To further elucidate the difference between the behaviour of test fragments in microwave and RF processing,  
232 the comparative individual thermal responses for each fragment in each ore sample are illustrated in Figure 6.  
233 Interestingly, the fragments in Ore 3 exhibit very similar thermal responses under microwave and RF  
234 treatment conditions. For Ores 2, 4 and 5, the thermal response for the majority of fragments falls within a  
235 similar range under both microwave and RF conditions, typically in the range 5-10°C. However for Ore 1 there  
236 are a significant number of fragments that have an average temperature rise below 1°C under microwave  
237 conditions, but a temperature rise between 2 and 6°C in the RF. There are also a small number of fragments  
238 in Ores 2, 4 and 5 that exhibit a significantly higher temperature rise in microwave processing compared to  
239 RF. These large differences in the very hottest fragments suggest a difference in the selective heating of  
240 mineral phases within these ore fragments between microwave and radio frequencies, for example a  
241 difference in thermal response of the hydrated clay minerals and sulphide minerals. These different thermal  
242 responses will be considered in more detail in Section 3.2.



243



244



245

246  
247

**Figure 6 Ore 1 (a), Ore 2 (b), Ore 3 (c), Ore 4 (d) and Ore 5 (e) individual fragment thermal responses, RF rotating packed bed and MW orientation 1**

248

249 **3.2 Comparing MW and RF ore sortability**

250 To determine whether radio frequency heating can provide a benefit over microwave heating for discrimination  
 251 between valuable and uneconomic fragments, the sortability of the same fragments under equivalent  
 252 conditions is compared. The metallurgical efficiency of any sorting process can be expressed as a curve  
 253 showing the (copper) recovery attainable at any value of mass recovery. The intrinsic sortability of an ore  
 254 sample is determined by ordering fragments from highest to lowest copper grade; cumulative recovery is then  
 255 determined on a fragment by fragment basis (Tucker et al., 2013). The actual sorting performance is  
 256 determined for both microwave and RF sorting by ordering the fragments according to individual fragment  
 257 average temperature rise, from coldest to hottest. The closer the actual curves are to the intrinsic curve, the  
 258 better the sorting performance.

259 S2 in the Supplementary Information illustrates the cumulative microwave and RF mass-copper sortability  
 260 curves alongside the intrinsic mass-copper curves for each ore sample tested. Sortability performance can be  
 261 readily determined from these curves by examining the copper recovery at different mass recoveries. Table 2  
 262 shows the intrinsic and actual microwave and RF rotating packed bed copper recoveries for each of the ores  
 263 tested, at 25%, 50% and 70% mass recoveries (copper recovery values represent the recovery at the  
 264 cumulative mass percentage for the fragments in each sample closest to the target mass recovery). Overall,  
 265 the copper recovery is higher under microwave conditions compared to rotating packed bed conditions, for the  
 266 majority of mass recoveries. It should be noted that whilst these arbitrary mass rejections are useful for  
 267 comparing different ores, and different discrimination technologies, sorting considerations for real operations  
 268 should be based on techno-economic considerations for a particular mine site. The optimisation of copper  
 269 recovery by tailoring temperature cut points in MW-IR sorting is addressed in (Batchelor et al., 2016). The  
 270 data presented here however indicates that there is no improvement in sortability performance using RF-  
 271 rotating packed beds compared to microwave sorting.

272

273 **Table 2 Intrinsic copper recoveries and actual microwave and RF rotating packed bed copper**  
 274 **recoveries at 25%, 50% and 75% mass recoveries**

	Mass Recovery %	Copper Recovery %		
		Intrinsic	MW	RF
<b>Ore 1</b>	<b>25</b>	49.3	25.9	29.1
	<b>50</b>	80.6	54.4	60.4
	<b>75</b>	94.0	91.2	76.4
<b>Ore 2</b>	<b>25</b>	53.0	36.0	29.9
	<b>50</b>	81.4	66.7	59.6
	<b>75</b>	96.1	86.2	85.4
<b>Ore 3</b>	<b>25</b>	64.0	12.5	9.7

	<b>50</b>	85.1	48.3	38.4
	<b>75</b>	94.0	65.2	64.5
<b>Ore 4</b>	<b>25</b>	59.5	38.1	46.9
	<b>50</b>	83.4	64.1	58.7
	<b>75</b>	95.6	90.5	87.5
<b>Ore 5</b>	<b>25</b>	62.2	27.8	14.1
	<b>50</b>	92.6	34.7	38.8
	<b>75</b>	98.8	79.8	73.9

275

276 Comparing selectivity in MW-IR and RF-IR sorting of ores

277 The differences in MW and RF sorting performance under equivalent conditions are most readily attributed to  
 278 a change in the selectivity of heating different mineral phases within the ores. (Batchelor et al., 2016) showed  
 279 that the main deviation from intrinsic sortability in microwave processing was due to the presence of iron  
 280 sulphides and hydrated clays, which also heat well when exposed to microwave energy. The mineral  
 281 conductivity measurements conducted by Genn and Morrison (2014) suggest a potential increase in  
 282 conductivity and therefore heating rate at radio frequencies for sulphide minerals. It is therefore necessary to  
 283 investigate whether changes in the relative heating of pyrite and chalcopyrite are responsible for lower copper  
 284 recoveries in RF compared to microwave sorting.

285 To determine the influence of the three principle heated phases (chalcopyrite, pyrite and moisture) in the ores  
 286 on the temperature rise of the fragments following microwave and RF treatment, multiple linear regressions  
 287 were run for each of the five ores. The fragment heating results for microwave treatments in orientation 1 and  
 288 orientation 2 were included as a single series to eliminate the effect of fragment orientation from the  
 289 regression analysis. Table 3 presents the P-value outputs from the regression analysis. A P-value of less than  
 290 5E-02 (0.05\*) is deemed to be statistically significant, whilst a value of less than 1E-03 (0.001\*\*) is statistically  
 291 highly significant.

292 **Table 3 Multiple linear regression P-values for significance of heated phase content on the average**  
 293 **surface temperature rise of fragments in ore samples following MW and RF rotating packed bed**  
 294 **treatment. \* significant, \*\* highly significant**

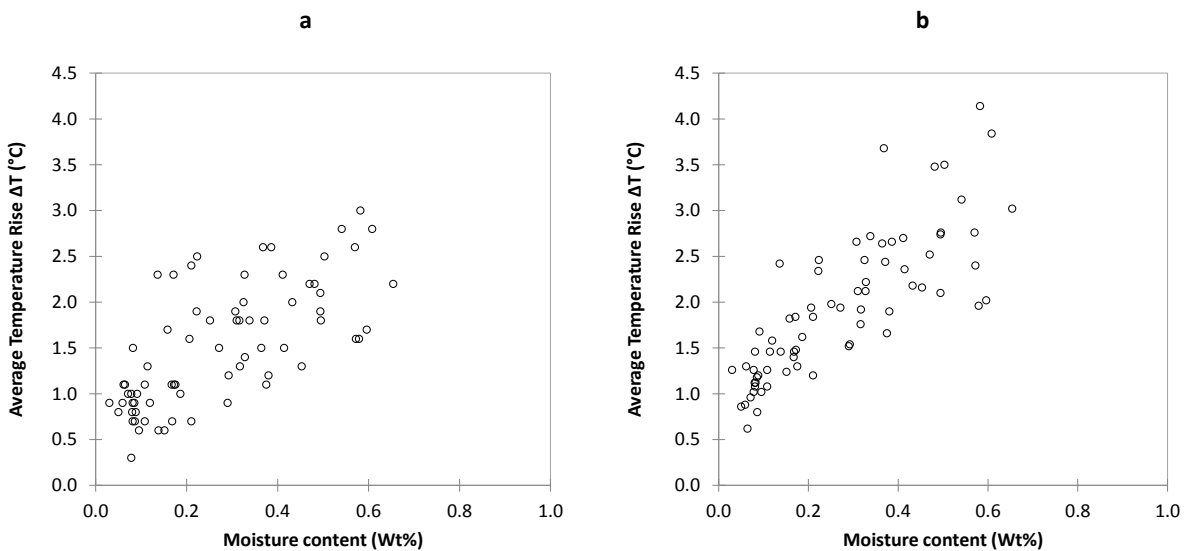
	<b>Ore 1</b>		<b>Ore 2</b>		<b>Ore 3</b>		<b>Ore 4</b>		<b>Ore 5</b>	
	MW	RF	MW	RF	MW	RF	MW	RF	MW	RF
<b>Chalcopyrite Weight%</b>	1.6x10 <sup>-1</sup>	6.9x10 <sup>-1</sup>	2.3x10 <sup>-3*</sup>	3.7x10 <sup>-3*</sup>	8.4x10 <sup>-2</sup>	5.3x10 <sup>-1</sup>	3.2x10 <sup>-1</sup>	1.7x10 <sup>-1</sup>	1.6x10 <sup>-3*</sup>	9.8x10 <sup>-2</sup>
<b>Pyrite Weight%</b>	4.6x10 <sup>-3*</sup>	8.5x10 <sup>-1</sup>	4.7x10 <sup>-1</sup>	4.4x10 <sup>-2*</sup>	9.8x10 <sup>-1</sup>	7.0x10 <sup>-1</sup>	1.1x10 <sup>-2*</sup>	3.1x10 <sup>-2*</sup>	1.6x10 <sup>-5**</sup>	9.9x10 <sup>-1</sup>
<b>Moisture Weight%</b>	4.8x10 <sup>-1</sup>	1.3x10 <sup>-5**</sup>	4.6x10 <sup>-12**</sup>	4.4x10 <sup>-19**</sup>	2.0x10 <sup>-25**</sup>	4.3x10 <sup>-32**</sup>	4.5x10 <sup>-14**</sup>	8.0x10 <sup>-4**</sup>	2.2x10 <sup>-27**</sup>	7.4x10 <sup>-44**</sup>

295

296 For all the samples with the exception of Ore 3, either chalcopyrite or pyrite content was found to have a  
 297 significant influence on individual fragment temperature rise in MW-IR sorting. It is noteworthy that the  
 298 chalcopyrite influence was generally less statistically significant than the pyrite content in MW heating.

299 Interestingly, moisture content was highly significant in the microwave treatment of all ores except ore 1; in  
300 this case the large pyrite content was dominant. This potential threshold for MW-IR sorting based on the  
301 content of different heating minerals is elucidated later in Section 4.

302 A major observation from these P-values is that in RF rotating packed bed processing, moisture content is  
303 statistically highly significant for every single ore, and more so than for microwave processing, with the  
304 exception of Ore 4. This suggests an increase in the selective heating of moisture within clay minerals at 27  
305 MHz compared to 896 MHz. This is exemplified in Figure 7 which illustrates the relationship between moisture  
306 content and individual fragment average temperature rise for microwave orientation 1 and RF rotating packed  
307 bed treatment at equivalent energy dose. As well as a tightening of the scatter in the trend between moisture  
308 content and temperature rise, there is an increase of between 20% and 30% in temperature rise for the hottest  
309 fragments in RF compared to microwave.

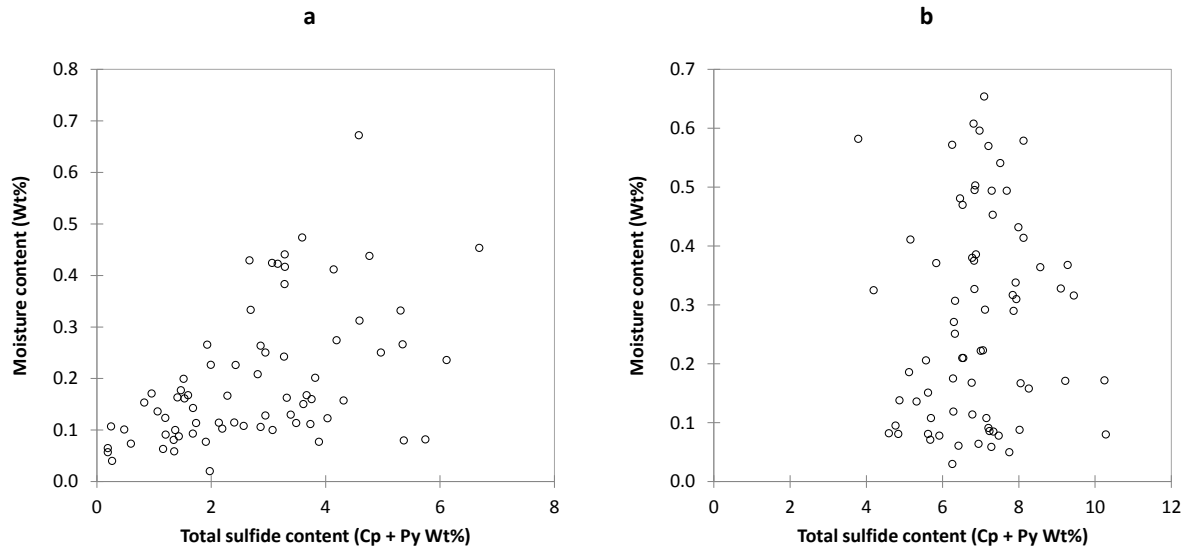


310

311 **Figure 7 Ore 3 microwave orientation 1 (a) and RF rotating packed bed (b) individual fragment thermal**  
312 **responses versus moisture content**



313 The P-values in Table 3 also show a clear reduction in the contribution of both pyrite and chalcopyrite to the  
314 heating of fragments during RF processing. It may be construed that there is a minor interaction between RF  
315 energy and sulphide minerals in Ore 2. However this can attributed to a degree of co-mineralisation between  
316 the sulphides and the hydrated minerals in some of the fragments; this is illustrated by the trends in Figure 8  
317 which show the individual fragment total sulphide content versus moisture content for Ore 2 and Ore 3, and  
318 indicate a correlation between sulphide and moisture in Ore 2, but not in Ore 3.



319

320 **Figure 8 Ore 2 (a) and Ore 3 (b) individual fragment total sulphide mineral content (chalcopyrite +**  
321 **pyrite weight %) versus moisture content (weight %)**

322 A full set of charts illustrating the relationship between temperature rise, sulphide content and moisture  
323 content for all five ores can be found in the Supplementary Information (S3-S7). Overall, these trends and P-  
324 values suggest that sulphide minerals do not interact at radio frequencies. The frequency dependence of  
325 electromagnetic properties is due to the relative contributions of different interaction mechanisms. However,  
326 dipolar rotation, ionic conduction and conductive losses all contribute to heating at both microwave and radio  
327 frequencies. Whilst differences in the relative contributions of these heating mechanisms are therefore  
328 expected, an absence of interaction at 27 MHz suggests another cause. A major difference between the RF  
329 and microwave systems is the absence of a significant magnetic field in the RF system; due to the parallel  
330 plate setup, the magnetic field is orders of magnitude smaller than the electric field. Therefore, any heating in  
331 RF is due predominantly to interaction with the electric field. It is proposed therefore that sulphide minerals in  
332 ores interact with the magnetic field at microwave frequencies. In figures S7-S11 in Supplementary  
333 Information, a small number of fragments exhibit a high increase in temperature in microwave processing that  
334 is not accounted for by either sulphide or moisture content. As these are not present in RF heating, it is  
335 possible that an unidentified heated phase interaction with the magnetic field is responsible. It was noted in  
336 (Batchelor et al., 2016) that a number of ore fragments tested contained weakly magnetic minerals such as

337 garnets, and strongly magnetic minerals such as magnetite. It is likely that these minerals, which due to their  
338 magnetic properties will interact strongly with magnetic fields, are the cause. This reinforces the need to  
339 understand the fundamental cause of these differences in selectivity between microwave and radio frequency.

## 340 **4 Understanding selectivity using synthetic fragments**

### 341 *4.1 Synthetic fragment fabrication*

342 To test the hypothesis that there is no significant interaction between sulphide minerals and electric fields in  
343 microwave and RF processing, synthetic fragments containing a single heated phase were produced. The  
344 synthetic particle transparent (non-heating) matrix was fabricated from polymethyl methacrylate (PMMA) and  
345 pulverised quartz using an adaptation of a method developed by Rizmanoski and Jokovic (2015) and  
346 previously used for validation of numerical modelling of ore fragment microwave heating (John et al., 2015).  
347 To produce a range of sulphide and clay contents, predetermined masses of -106+75 µm pyrite grains  
348 (purchased as lump pyrite from Gregory Bottley and Lloyd) or nominally -106 micron analytical grade  
349 montmorillonite powder were blended with the matrix mixture until homogenised. This even dissemination  
350 throughout the matrix minimised any heating effects due to texture. Thermogravimetric analysis of pure  
351 montmorillonite showed that the mineral contained 9.4%wt free water and 3.5%wt bound water, giving a total  
352 moisture content of 12.9%wt. Four fragments of each pyrite/montmorillonite grade were made to determine  
353 variations due to difference in electromagnetic field exposure in individual fragments of similar 'mineralogy'. A  
354 set of barren fragments (no pyrite or montmorillonite) was also produced to provide a baseline for comparison.  
355 The mixture for each set of 'identical' fragments was formed by hand into round fragments of approximately  
356 30mm diameter, with an average mass of 25g. This rounded geometry allowed fragments to be treated as a  
357 monolayer in RF testing without significant shape effects observed in the RF monolayer heating of angular  
358 real ore fragments.

### 359 *4.2 Synthetic fragment microwave and RF testing*

360 Microwave treatment of synthetic fragments was conducted in a 2450 MHz multimode cavity and in the 27  
361 MHz RF system, at an equivalent target dose of approximately 4 kWh/t. Although this dose is significantly  
362 higher than the economic 0.5-1.0 kWh/t target for EM energy dose in MW-IR sorting testing completed thus  
363 far, it was selected to allow any potential temperature rises of sulphides in the RF system to be distinguishable  
364 from background heating of the matrix.

365 For microwave testing, 8 fragments were placed around the edge of the plastic disc and placed under the  
366 thermal camera for cold imaging. The disc was then placed on the microwave turntable and heated the  
367 fragments treated for 5 seconds at 1.1kW applied power. Assuming all energy was absorbed, the  
368 comparative dose was approximately 4.4kWh/t across all tests. For 27 MHz RF monolayer testing, fragments

369 were placed in plastic trays on the conveyor belt. The samples were then treated at 5kW applied power for  
 370 20s giving an overall comparative dose of 4.3kWh/t across all tests.

### 371 4.3 Synthetic fragment results

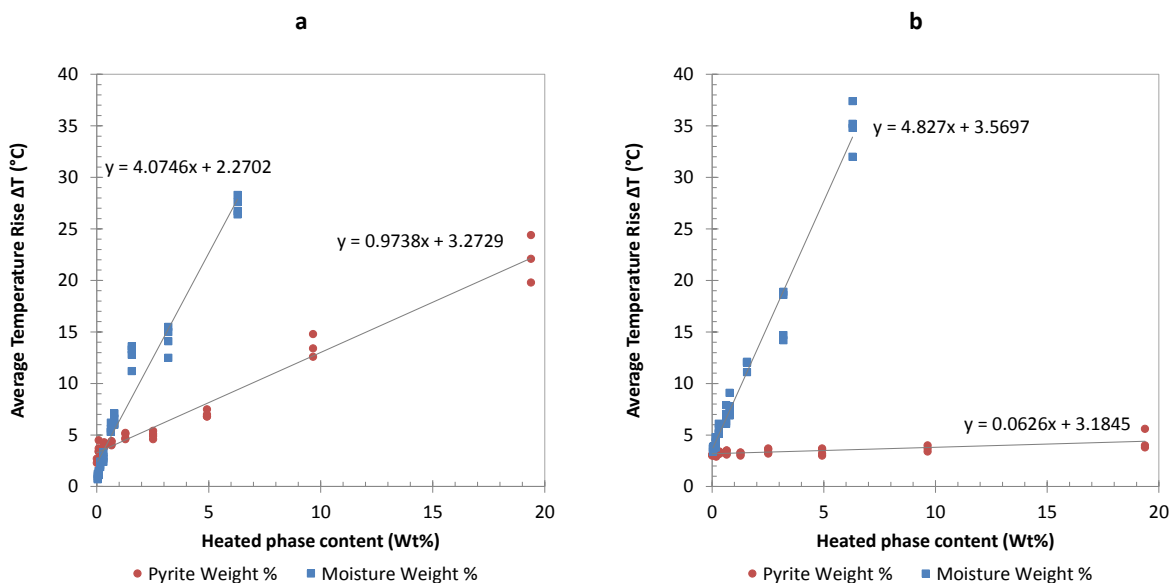
372 Multiple linear regression analysis was run to determine the significance of microwave-heating phase content  
 373 on the average surface temperature rise of synthetic fragments following batch monolayer microwave and RF  
 374 treatment. Table 4 presents the P-value outputs from the regression analysis.

375 **Table 4 Multiple linear regression P-values for significance of heated phase content on the average**  
 376 **surface temperature rise of fragments in synthetic fragments following batch MW and RF monolayer**  
 377 **treatment. \* significant, \*\* highly significant**

Synthetic fragments	Batch MW	RF Monolayer
Pyrite Weight%	$1.6 \times 10^{-35}$ **	$1.1 \times 10^{-01}$
Moisture Weight%	$2.7 \times 10^{-45}$ **	$1.5 \times 10^{-61}$ **

378

379 As expected, both pyrite and moisture content have a statistically highly significant influence on the average  
 380 temperature rise from microwave heating. However, there was no influence of pyrite content on temperature  
 381 rise in RF heating. Figure 9 illustrates the individual synthetic fragment average temperature versus heated  
 382 phase content following microwave and RF heating at equivalent energy dose of ~4.4kWh/t. The spread  
 383 observed in the temperature rise of 'identical' fragments can be attributed to slight variations in fragment  
 384 mass, shape, grade and absorbent phase distribution, all of which have previously been shown in previous  
 385 work to have minor contributions to average temperature rise (John et al., 2015, Batchelor et al., 2016)



386

387 **Figure 9 Microwave monolayer (a) and RF monolayer (b) individual pyrite and montmorillonite**  
 388 **(moisture) containing synthetic fragment thermal responses, batch 4.3-4.4 kWh/t, and linear models**

389 Applying the linear models in Figure 9a for the microwave heating of synthetic fragments with pyrite and  
 390 moisture contents between 1 and 10 weight % indicates that at equivalent heated phase content the

391 temperature rise of the moisture (montmorillonite clay) containing fragments is 2.5 times that of pyrite  
 392 containing fragments. Comparison of the linear models for temperature increase of montmorillonite containing  
 393 synthetic fragments (again between 1 and 10 weight %) shows that for the same moisture content, the  
 394 average increase in temperature is 25% higher in RF compared to microwave treatment. This again is an  
 395 indication of increased selectivity in the heating of adsorbed interlayer water in the montmorillonite clay, as  
 396 was seen in the heating of the real ore fragments. In RF heating, there is no discernible correlation between  
 397 temperature rise and pyrite content. Furthermore, there is no significant temperature rise for the highest pyrite  
 398 content fragments compared to the lower pyrite content fragments. This suggests that pyrite exhibits little or  
 399 no heating in radio frequency systems at 27 MHz. This is a significant result and supports the proposal that  
 400 semi conducting sulphide minerals heat in microwave systems via interaction with the magnetic field: in the  
 401 RF system there is predominantly electric field between the RF electrodes. This explains why there were  
 402 significant differences in the MW and RF heating profiles of low moisture-high sulphide fragments during  
 403 testing of real ores.

404 The electromagnetic effects behind this type of behaviour in other conducting materials have been recently  
 405 demonstrated by Porch et al. (2013). Generally, small conducting particles will heat rapidly when placed in a  
 406 microwave field, limited only by the skin depth of the material (the depth at which the current density is equal  
 407 to 1/e of the surface value (Meredith, 1998)). However, the internal electric field within these conducting  
 408 particles is highly screened due to surface charges. Porch's investigation of the microwave absorption  
 409 behaviour of small (non-magnetic) conducting particles showed that induction heating caused by eddy  
 410 currents associated with the magnetic field is responsible for heating and was maximised at specific particle  
 411 radii. For non-conducting and weakly-conducting particles, electric dipole induced heating is dominant, and  
 412 maximised at specific conductivities relative to electromagnetic frequency. A summary of these limitations is  
 413 shown in Table 5. A full derivation and background to these results are covered in detail in Porch et al. (2013).

414 **Table 5 Electromagnetic heating factors and limitations for non-magnetic semi-conducting ore mineral**  
 415 **particles,  $\sigma > 0.1$  S/m, particle radius  $1\text{nm} < a < 1\text{mm}$ . Adapted from Porch et al. (2013)**

Field	Microwave heating (f =2.45 GHz)	RF parallel plate heating (f =27.12 MHz)
Electric	Limited by screening. Maximum absorption when: $\sigma \approx \omega \epsilon_0$	
Magnetic	Limited by skin depth: $\delta_s = \left(\frac{2}{\sigma \omega \mu_0}\right)^{0.5}$ Maximum absorption where: $a = 2.41 \delta_s$	n/a minimal magnetic field present

416 Where  $\delta_s$  = skin depth (m);  $\sigma$  = electrical conductivity of the material (S/m); f= frequency (Hz);  $\omega$  = angular frequency ( $2\pi f$  rad/s);  $\epsilon_0$ =permittivity of  
 417 free space ( $8.854 \times 10^{-12}$  F/m);  $\mu_0$  = permeability of free space ( $4\pi \times 10^{-7}$  m.kg/C<sup>2</sup>).

418

419 Literature values for the conductivities of natural sulphide minerals such as pyrite and chalcopyrite have been  
420 reported between 1.0 and  $1 \times 10^5$  S/m (Pridmore and Shuey, 1976) with variations ascribed to differences in  
421 stoichiometry (Harvey, 1928, Parasnis, 1956) or the presence and concentration of impurities (Shuey, 1975).  
422 Given this range of values, it is perhaps not unexpected that these semi-conducting minerals could behave  
423 either closer to insulators or conductors depending on their (ore deposit specific) properties. Therefore,  
424 heating of semi-conducting minerals in RF at the grain sizes typically seen in porphyry copper ores can be  
425 extremely low, due to screening of the electric field and minimal magnetic field.

426 As well as elucidating how semi-conducting sulphide minerals may interact with electromagnetic fields during  
427 microwave processing applications, these results also highlight the threshold ratio of sulphides and clays  
428 required to provide even heating due to each mineral group at 2.45 GHz (assuming that all clays heat equally  
429 and all sulphides heat equally). Approximately 2.5 times the mass of sulphide to clay would result in equal  
430 temperature rises for fragments in which the microwave-heating minerals were evenly disseminated through  
431 the matrix. This understanding can aid in the selection of ores which could potentially be the most amenable  
432 to MW-IR sorting. Overall, low hydrated clay content ores with copper sulphides as the main sulphide, or with  
433 a high degree of co-mineralisation between copper and iron sulphides, present the best case for sorting at  
434 near intrinsic sortability using MW-IR. The application of RF-IR to sorting of mined materials has promise for  
435 applications where pure dielectric sorting is required (such as in the discrimination of high and low moisture  
436 materials) or where the conductivity of sulphide ore minerals is sufficiently low that electric field screening  
437 does not inhibit heating. To fully understand the amenability of any ore or material to MW-IR or RF-IR sorting,  
438 full characterisation of all heating phases and their relative weighted contributions to individual fragment  
439 heating is required in future test programmes.

440

441 **5 Conclusions**

442 Radio frequency heating followed by infra-red thermal imaging has been investigated as an excitation-  
443 discrimination technique for sorting of ores. By developing a novel presentation and bulk handling method to  
444 allow even heating of fragments within a pilot scale parallel plate RF system, the fragment-by-fragment  
445 thermal response of a number of ore samples and synthetic fragments has been evaluated and compared to  
446 microwave treatment at pilot and batch scales. It has been shown that there is an increase in the selectivity of  
447 the heating of hydrated clay minerals at RF compared to microwave frequencies. Significantly, it has been  
448 shown that heating of semi-conducting sulphide minerals at radio frequencies is limited by electric field  
449 screening. It is suggested that the interaction of these minerals at microwave frequencies is likely to be due to  
450 induction heating via eddy currents associated with the magnetic field component. Whilst RF-IR is not a viable  
451 technique for sorting of the porphyry copper ores tested here, it could find applications where sorting or  
452 grading of material based on moisture content is required. Thermal response profiles of synthetic fragments  
453 have shown that hydrated clay minerals heat approximately 2.5 times as much as sulphides at microwave  
454 frequencies for the minerals tested. Conductivity is suggested to be a key to determining the relative  
455 absorption of electric and magnetic fields and ultimately the heating response of semi-conducting minerals.  
456 The amenability of different ores and mine sites to both microwave and radio frequency IR sorting will be best  
457 determined in future through thorough characterisation of mineral electrical and magnetic properties, and via  
458 the development of statistical models that incorporate thermal response weighting of heated phase content,  
459 together with textural, geometric and process variables.

460

461

462 **Acknowledgements**

463 We greatly acknowledge Rio Tinto Technology and Innovation along with their research and industry partners  
464 for engagement and collaboration throughout the Copper NuWave™ project. The authors would also like to  
465 thank the technical staff of the Microwave Process Engineering Group at the University of Nottingham:  
466 Richard Meehan, Joe Meehan, Rachael Baines, Matt Rus, Matt Nicholls, and Richard Thompson, and the  
467 JKMRRC at the University of Queensland for preparing ore samples for testing.

468

469

- 471 BATCHELOR, A. R., FERRARI-JOHN, R. S., KATRIB, J., UDOUDO, O., JONES, D. A., DODDS, C. &  
472 KINGMAN, S. W. 2016. Pilot scale microwave sorting of porphyry copper ores: Part 1 – Laboratory  
473 investigations. *Minerals Engineering*.
- 474 CHUNPENG, L. & YIXIN, H. 1996. HEATING RATE OF MINERALS AND COMPOUNDS IN MICROWAVE FIELD.  
475 FERRARI-JOHN, R. S., KATRIB, J., PALADE, P., BATCHELOR, A. R., DODDS, C. & KINGMAN, S. W. 2016. A  
476 Tool for Predicting Heating Uniformity in Industrial Radio Frequency Processing. *Food and*  
477 *Bioprocess Technology*, 1-9.
- 478 GENN, G. & MORRISON, R. 2014. Mineral conductivity measurements. *Minerals Engineering*.
- 479 GHOSH, A., NAYAK, B., DAS, T. & PALIT SAGAR, S. 2013. A non-invasive technique for sorting of alumina-  
480 rich iron ores. *Minerals Engineering*, 45, 55-58.
- 481 GHOSH, A., SHARMA, A., NAYAK, B. & SAGAR, S. P. 2014. Infrared thermography: An approach for iron  
482 ore gradation. *Minerals Engineering*.
- 483 HARRISON, P. C. 1997. *A fundamental study of the heating effect of 2.45 GHz radiation on minerals*. PhD,  
484 University of Birmingham.
- 485 HARVEY, R. D. 1928. Electrical conductivity and polished mineral surfaces. *Economic Geology*, 23, 778-  
486 803.
- 487 JOHN, R. S., BATCHELOR, A. R., IVANOV, D., UDOUDO, O. B., JONES, D. A., DODDS, C. & KINGMAN, S.  
488 W. 2015. Understanding microwave induced sorting of porphyry copper ores. *Minerals Engineering*,  
489 84, 77-87.
- 490 KLEIN, B. & MAZHARY, A. 2015. Heterogeneity of Low-Grade Ores and Amenability to Sensor-Based  
491 Sorting. *CMP 2015*.
- 492 LESSARD, J., DE BAKKER, J. & MCHUGH, L. 2014. Development of ore sorting and its impact on mineral  
493 processing economics. *Minerals Engineering*, 65, 88-97.
- 494 MCGILL, S., WALKIEWICZ, J. W. & CLARK, A. 1995. *Microwave Heating of Chemicals and Minerals*, US  
495 Department of the Interior, Bureau of Mines.
- 496 MEREDITH, R. J. 1998. *Engineers' Handbook of Industrial Microwave Heating*, Institution of Electrical  
497 Engineers.
- 498 NORGATE, T. & JAHANSHAHI, S. 2010. Low grade ores–Smelt, leach or concentrate? *Minerals Engineering*,  
499 23, 65-73.
- 500 PARASNIS, D. 1956. The electrical resistivity of some sulphide and oxide minerals and their ores.  
501 *Geophysical prospecting*, 4, 249-278.
- 502 POKRAJIC, Z., MORRISON, R. & JOHNSON, B. Designing for a reduced carbon footprint at Greenfield and  
503 operating comminution plants. Recent Advances in Mineral Processing Plant Design, 2009. Society  
504 for Mining, Metallurgy, and Exploration, 560-570.
- 505 PORCH, A., SLOCOMBE, D. & EDWARDS, P. P. 2013. Microwave absorption in powders of small conducting  
506 particles for heating applications. *Physical Chemistry Chemical Physics*, 15, 2757-2763.
- 507 PRIDMORE, D. & SHUEY, R. 1976. The electrical resistivity of galena, pyrite, and chalcopyrite. *American*  
508 *Mineralogist*, 61, 248-259.
- 509 RADIOMETRIC INFRARED SOLUTIONS 2011. Radiometric Complete 5.1 Manual
- 510 RIZMANOSKI, V. & JOKOVIC, V. 2015. Synthetic Ore Samples to Test Microwave/RF Applicators and  
511 Processes. *Journal of Materials Processing Technology*.
- 512 SALTER, J. D. & WYATT, N. P. G. 1991. Sorting in the minerals industry: Past, present and future. *Minerals*  
513 *Engineering*, 4, 779-796.
- 514 SHUEY, R. T. 1975. *Semi-Conducting Ore Minerals*, Elsevier Scientific Publishing Company.
- 515 TONG, L., KHOSHABA, B., BAMBER, A. & KLEIN, B. 2015. Correlation and regression analysis in the X-ray  
516 fluorescence sorting of a low grade copper ore *SAG Conference*.
- 517 TUCKER, J., MORRISON, R. & WELLWOOD, G. The development of indices to assess both the sorting  
518 potential of an ore and the performance of any sorting process when treating that ore. Physical  
519 Separation'13, 2013. Minerals Engineering International, 1-12.
- 520 VAN BERKEL, R. 2007. Eco-efficiency in primary metals production: Context, perspectives and methods.  
521 *Resources, Conservation and Recycling*, 51, 511-540.
- 522 VAN WEERT, G. & KONDOS, P. 2008. Effects of susceptor size and concentration on the efficiency of  
523 microwave/infrared (MW/IR) sorting. *CIM Journal*, 2.
- 524 VAN WEERT, G., KONDOS, P. & WANG, O. 2011. Microwave heating of sulphide minerals as a function of  
525 their size and spatial distribution. *CIM Journal*, 2.
- 526 WALKIEWICZ, J. W. K., G. ; MCGILL, S. L. 1988. *Microwave heating characteristics of selected minerals*  
527 *and compounds*.
- 528 WILLS, B. A., NAPIER-MUNN, T. & CENTRE, J. K. M. R. 2006. *Wills' mineral processing technology: an*  
529 *introduction to the practical aspects of ore treatment and mineral recovery*, Elsevier/BH.
- 530  
531